Journal of Automation and Intelligence 4 (2025) 108–114

Contents lists available at ScienceDirect

Journal of Automation and Intelligence

Research Article

Group formation tracking for heterogeneous linear multi-agent systems under switching topologies

Shiyu Zhou *, Dong Sun

Department of Biomedical Engineering, City University of Hong Kong, Hong Kong, 999077, China

ARTICLE INFO

Keywords:
Formation tracking
Group division
Switching topologies
Multi-agent systems

ABSTRACT

This article investigates the time-varying output group formation tracking control (GFTC) problem for heterogeneous multi-agent systems (HMASs) under switching topologies. The objective is to design a distributed control strategy that enables the outputs of the followers to form the desired sub-formations and track the outputs of the leader in each subgroup. Firstly, novel distributed observers are developed to estimate the states of the leaders under switching topologies. Then, GFTC protocols are designed based on the proposed observers. It is shown that with the distributed protocol, the GFTC problem for HMASs under switching topologies is solved if the average dwell time associated with the switching topologies is larger than a fixed threshold. Finally, an example is provided to illustrate the effectiveness of the proposed control strategy.

1. Introduction

Formation control of multi-agent systems (MASs) has attracted significant attention over recent decades due to its wide range of applications, such as agricultural monitoring, delivery services, and disaster management [1–3]. Consensus-based formation control, as a typical class of consensus control, can significantly reduce communication costs and improve the robustness of the system [4]. Some relevant works on consensus-based formation control can be found in [5–7].

In practice, MASs are required to achieve the desired formation and simultaneously track a reference trajectory provided by an exosystem. For instance, in agricultural monitoring applications, leader drones equipped with advanced sensors will navigate over farmlands to collect essential data, such as crop health and soil conditions. The follower drones can maintain a specific shape while tracking the trajectory of the leaders, allowing them to cover a wider area and collect supplementary data. This gives rise to the so-called time-varying formation tracking control problem. Numerous formation tracking control problems have been investigated for homogeneous MASs [8–12]. However, the dynamics of agents are often different in practice. These systems are referred to as heterogeneous multi-agent systems (HMASs). Recently, extensive research has been conducted on formation tracking control problems for HMASs [13–15].

In practical applications, it is often necessary to coordinate multiple groups of agents. Take, for instance, the fire rescue scenario depicted in Fig. 1, where the heterogeneous MASs consisting of quadrotors and unmanned ground vehicles are organized into several groups. Each group forms a specific formation and is assigned to reach different fire locations. Consequently, group cooperative control problems of MASs have attracted considerable attention, including group consensus, group formation, and group formation tracking (see, for example, [16–21]). The group formation control problem for MASs was investigated in [19], where the feasibility condition for achieving the time-varying formation was also presented. The group formation tracking containment control problem for MASs was investigated in [20]. In contrast to studies focused on homogeneous MASs [16–20], the group formation tracking control (GFTC) problem for HMASs was studied in [21].

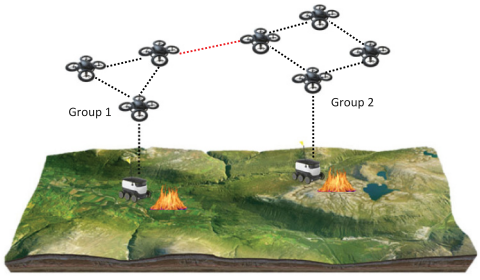

Fig. 1. The schematic diagram of fire rescue.

It is worth noting that the aforementioned studies [16–21] primarily focus on achieving cooperative control under a fixed interaction topology. However, due to a range of factors, such as obstructions or failures in communication device links, switching topologies often become inevitable in most real-world applications. Therefore, the investigation of cooperative control of MASs under switching topologies has received considerable attention, such as consensus problems [22,23], formation control problems [24,25], and group coordination problems [26–28]. The time-varying formation tracking problem for MASs with undirected switching graphs was studied in [25], where all graphs were required to have a spanning tree. The group consensus problem for general linear MASs with and without switching topologies was investigated in [27]. In [28], the GFTC problem with switching networks was studied; however, it focused on homogeneous system dynamics and did not consider cooperation among different subgroups. To the best of our knowledge, the problem of GFTC for HMASs with switching topologies is still open, which motivates this study.

In this paper, the time-varying output GFTC problem for HMASs with switching topologies is investigated. To this end, we initially develop novel distributed observers for each follower to estimate the state of the leader in each subgroup under switching topologies. Subsequently, the GFTC protocols are proposed to ensure that the followers in each subgroup achieve the desired formation and track the trajectory provided by their respective leaders. The main contributions of this study are summarized as follows:

1. A novel distributed observer is first introduced by considering both inter-group and intra-group interactions, enabling the estimation of states for leaders under switching topologies. Subsequently, an observer-based distributed controller is developed so that the GFTC problem can be solved. Considering that multiple groups can be seen as the extension of a single group, our proposed method encompasses several existing formation tracking control methods such as those in [13–15] as special instances.
2. This work considers the GFTC problem for MASs with general heterogeneous dynamics, which encompass first-order or second-order dynamics studied in [26], as well as homogeneous agent dynamics investigated in [27,28] as special cases.
3. Different from the previous studies on group cooperative problems for MASs that do not consider switching topologies [16–21], this research focuses on the GFTC problem for HMASs with switching topologies. The ability to adapt to varying interaction topologies enables our method to manage more complex and diverse networks effectively.

This paper is structured as follows: Section 2 provides some preliminaries and formulates the GFTC problem. In Section 3, the distributed controllers and the analysis of closed-loop systems are presented. Section 4 demonstrates the effectiveness of the proposed control strategy through a numerical example. Finally, Section 5 concludes this paper.

Notations. $\mathbf{0}_{p\times q}$ and $\mathbf{1}_{p\times q}$ represent the $p\times q$ matrices where all elements are zero and one, respectively. The n dimensional identity matrix is denoted by I_n. $\otimes$ and $\|\cdot\|$ represent the Kronecker product and the Euclidean norm. The diagonal block matrix is defined as $\mathrm{diag}\{v_1,\ldots,v_i,\ldots,v_k\}$ with v_i as its diagonal entry. The functions $\min\{\cdot\}$ and $\max\{\cdot\}$ determine the minimum and maximum elements of an array, respectively. For a matrix $\mathcal{A}\in\mathbb{R}^{n\times n}$ with all the eigenvalues being real, $\lambda_{\max}(\mathcal{A})$ and $\lambda_{\min}(\mathcal{A})$ denote the largest and smallest eigenvalues of $\mathcal{A}$, respectively.

2. Preliminaries and problem formulation

2.1. Preliminaries

Considers a HMAS consisting of N_f followers and N_l leaders. An agent is defined as a leader if it does not have any neighboring agents; conversely, it is classified as a follower if it has at least one neighboring agent. Define $\mathcal{G}_f=\left(\mathcal{O}_f,\mathcal{E}_f,\mathcal{A}_f\right)$ as a directed graph among followers, where $\mathcal{O}_f=\left\{1,\ldots,N_f\right\}$ represents a set of nodes, $\mathcal{E}_f$ denotes the set of edges, and $\mathcal{A}_f=[a_{ij}]\in\mathbb{R}^{N_f\times N_f}$ represents the weighted adjacency matrix with $a_{ij}>0$ if $(j,i)\in\mathcal{E}_f$, and $a_{ij}=0$ otherwise. The pinning gains from the kth leader to each follower i are represented by a_{i0k}, where $a_{i0k}>0$ indicates the capability of information transmission from the leader k to the follower i; otherwise, $a_{i0k}=0$. A spanning tree is a directed graph where at least one root node possesses a directed path connecting it to all other nodes.

The HMAS is partitioned into N_l subgroups denoted as $\mathcal{O}_k, k=1,\ldots,N_l$, each consisting of one leader and g_i followers, with $\sum_{i=1}^{N_l}g_i=N_f$. Let $\mathcal{O}_l=\{1,\ldots,N_l\}$ denote the set of the leaders. The partition of $\mathcal{O}_f$ is defined as $\{\mathcal{O}_{f1},\mathcal{O}_{f2},\ldots,\mathcal{O}_{fN_l}\}$ satisfying $\mathcal{O}_{fj}\neq\varnothing\left(j=1,\ldots,N_l\right)$, $\cup_{j=1}^{N_l}\mathcal{O}_{fj}=\mathcal{O}_f$, and $\mathcal{O}_{fj}\cap\mathcal{O}_{fs}=\varnothing\left(j,s\in\{1,2,\ldots,N_l\}\ ;\ j\neq s\right)$. It can be seen that $\mathcal{O}_k$ consists of the kth leader and the subset of followers $\mathcal{O}_{fk}$.

Let $\sigma(t):[0,+\infty)\to\{1,\ldots,s\}$ be the piecewise switching signal. Consider an infinite sequence of uniformly bounded, non-overlapping time intervals $[t_h,t_{h+1})$ with $h\in\mathbb{N}$ and $t_1=0$. Each interval satisfies $0<\tau_d\le t_{h+1}-t_h$, where τ_d is referred to as the dwell time. It is important to note that within this paper, the communication graph remains fixed during each time interval and changes only at the switching time t_{h+1}.

Definition 1 ([29]). During any time interval (T_m,T_n) with $T_n>T_m>0$, if the number of switches $N_{\sigma(T_m,T_n)}$ satisfies $N_{\sigma(T_m,T_n)}\le N_0+\frac{T_n-T_m}{\bar{\tau}_d}$, where N_0 and $\bar{\tau}$ are positive constants, $\bar{\tau}_d$ is defined as the average dwell time of the signal $\sigma(t)$.

Let $\mathcal{G}^{\sigma(t)}$ be the switching digraph, and the corresponding Laplacian matrix is defined as $\mathcal{L}^{\sigma(t)}=\begin{bmatrix}\mathcal{L}_1^{\sigma(t)} & \mathcal{L}_2^{\sigma(t)}\\ \mathbf{0}_{N_l\times N_f} & \mathbf{0}_{N_l\times N_l}\end{bmatrix}$, where $\mathcal{L}_2^{\sigma(t)}=\left[-a_{0ik}^{\sigma(t)}\right]_{N_f\times N_l}$, $\mathcal{L}_1^{\sigma(t)}=\left[l_{ij}^{\sigma(t)}\right]_{N_f\times N_f}$ with $l_{ij}^{\sigma(t)}=-a_{ij}^{\sigma(t)}$ for $i\neq j$, and $l_{ij}=\sum_{m=1}^{N_f}a_{im}^{\sigma(t)}+\sum_{k=1}^{N_l}a_{i0k}^{\sigma(t)}$ for $i=j$.

2.2. Problem formulation

The dynamics of the ith $\left(i\in\mathcal{O}_f\right)$ follower is given as:

$$\begin{aligned}\dot{\boldsymbol{x}}_i(t)=&\boldsymbol{A}_i\boldsymbol{x}_i(t)+\boldsymbol{B}_i\boldsymbol{u}_i(t),\\ \boldsymbol{y}_i(t)=&\boldsymbol{C}_i\boldsymbol{x}_i(t),\end{aligned}\tag{1}$$

where $\boldsymbol{x}_i\in\mathbb{R}^{n_i}$, $\boldsymbol{u}_i\in\mathbb{R}^{m_i}$, $\boldsymbol{y}_i\in\mathbb{R}^{p}$ represent the state, control input, and output of the ith follower, respectively, $\boldsymbol{A}_i\in\mathbb{R}^{n_i\times n_i}$, $\boldsymbol{B}_i\in\mathbb{R}^{n_i\times m_i}$, and $\boldsymbol{C}_i\in\mathbb{R}^{p\times n_i}$ are the system matrices.

The model of the ith $\left(i\in\mathcal{O}_l\right)$ leader is given as:

$$\begin{aligned}\dot{\boldsymbol{x}}_{0i}(t)=&\boldsymbol{A}_0\boldsymbol{x}_{0i}(t),\\ \boldsymbol{y}_{0i}(t)=&\boldsymbol{C}_0\boldsymbol{x}_{0i}(t),\end{aligned}\tag{2}$$

where $\boldsymbol{x}_{0i}\in\mathbb{R}^{n_0}$, and $\boldsymbol{y}_{0i}\in\mathbb{R}^{p}$ represent the state and output of the leader, respectively, $\boldsymbol{A}_0\in\mathbb{R}^{n_0\times n_0}$ and $\boldsymbol{C}_0\in\mathbb{R}^{p\times n_0}$ are the system matrices of the leader.

This paper investigates the GFTC problem with switching topologies. For any subgroup $\mathcal{O}_q=\{\text{leader } q,\mathcal{O}_{fq}\}$ $(q=1,\ldots,N_l)$, let $\boldsymbol{h}_{xi}(t)\in\mathbb{R}^{n_0}$ represent the piecewise continuous differentiable time-varying formation vector satisfying

$$\begin{aligned}\dot{\boldsymbol{h}}_{xi}(t)=&\boldsymbol{A}_F\boldsymbol{h}_{xi},\\ \boldsymbol{h}_{yi}(t)=&\boldsymbol{C}_F\boldsymbol{h}_{xi},\end{aligned}\tag{3}$$

where $\boldsymbol{h}_{yi}\in\mathbb{R}^{p}$, $\boldsymbol{A}_F$ and $\boldsymbol{C}_F$ are matrices of compatible dimensions. Then, the GFTC problem with switching topologies is formulated as follows.

Remark 1. A variety of formation shapes can be generated by Eq. (3), such as time-invariant formation [30], three-dimensional formation [25,31,32], and scaling formation [33]. Specifically, by setting $A_h = \mathbf{0}_{n_0\times n_0}$ and $C_h = \mathrm{I}_{p\times n_0}$, this equation can specify the non-rotating time-invariant formation shape. Additionally, the three-dimensional formation shape in [25,31,32] can be generate by setting $A_h = \begin{pmatrix} 0 & 1 \\ -c^2 & 0 \end{pmatrix}$ and $C_h = \begin{pmatrix} 1 & 0 \end{pmatrix}$ along each of the X, Y, and Z axes, respectively, where c represents a positive constant.

Definition 2 (*GFTC Problem*). Consider HMAS consisting of (1) and (2) with switching topologies $\mathcal{G}^{\sigma(t)}$. The GFTC problem can be solved if there exists a distributed protocol for each follower in any subgroup $\mathcal{O}_q = \{\text{leader } q, \mathcal{O}_{fq}\}$, $q = 1,\dots,N_l$, such that

$$\lim_{t\to+\infty} \|\boldsymbol{y}_i(t) - \boldsymbol{h}_{yi}(t) - \boldsymbol{y}_{0k}(t)\| = 0,\ \forall i \in \mathcal{O}_{fq}. \tag{4}$$

Before proceeding further, the following Assumptions and Lemmas are introduced.

Assumption 1. For any $i \in \mathcal{O}_f$, $(\boldsymbol{A}_i, \boldsymbol{B}_i)$ are stabilizable, and $(\boldsymbol{C}_i, \boldsymbol{A}_i)$ are detectable.

Assumption 2. The following regulator equations,

$$\begin{aligned} \boldsymbol{X}_i\boldsymbol{A}_0 &= \boldsymbol{A}_i\boldsymbol{X}_i + \boldsymbol{B}_i\boldsymbol{U}_i, \\ 0 &= \boldsymbol{C}_i\boldsymbol{X}_i - \boldsymbol{C}_0, \end{aligned} \tag{5}$$

have solution pairs $(\boldsymbol{X}_i, \boldsymbol{U}_i)$ for all $i \in \mathcal{O}_f$.

Assumption 3. The following linear matrix equations,

$$\begin{aligned} \boldsymbol{X}_{Fi}\boldsymbol{A}_F &= \boldsymbol{A}_i\boldsymbol{X}_{Fi} + \boldsymbol{B}_i\boldsymbol{U}_{Fi}, \\ 0 &= \boldsymbol{C}_i\boldsymbol{X}_{Fi} - \boldsymbol{C}_F, \end{aligned} \tag{6}$$

have solution pairs $(\boldsymbol{X}_{Fi}, \boldsymbol{U}_{Fi})$ for all $i \in \mathcal{O}_f$.

Assumption 4. The partition $\{\mathcal{O}_{f1}, \mathcal{O}_{f2}, \dots, \mathcal{O}_{fN_l}\}$ is an acyclic partition for the set of followers $\mathcal{O}_f$.

It follows from Assumptions 4 that $\mathcal{L}_1^{\sigma(t)}$ has the following form [27]

$$\mathcal{L}_1^{\sigma(t)} = \begin{bmatrix} \mathcal{L}_{g_1}^{\sigma(t)} & \mathbf{0}_{g_1\times g_2} & \cdots & \mathbf{0}_{g_1\times g_N} \\ \mathcal{L}_{g_{21}}^{\sigma(t)} & \ddots & & \mathbf{0}_{g_2\times g_N} \\ \vdots & \mathcal{L}_{g_{ij}}^{\sigma(t)} & \ddots & \vdots \\ \mathcal{L}_{g_{N1}}^{\sigma(t)} & \cdots & \cdots & \mathcal{L}_{g_N}^{\sigma(t)} \end{bmatrix},$$

where $\mathcal{L}_{g_i}^{\sigma(t)}$ represents the switching interaction among the agents in subgroup $\mathcal{O}_i$. The switching interaction between the followers of subgroups $\mathcal{O}_i$ and $\mathcal{O}_j$ is defined as $\mathcal{L}_{g_{ij}}^{\sigma(t)}$.

Assumption 5. For any subgroup $\mathcal{O}_q = \{\text{leader } k, \mathcal{O}_{fk}\}$, the corresponding switching communication topology contains a spanning tree with the kth leader as its root node.

Assumption 6. For any given subgroups $\mathcal{O}_i$ and $\mathcal{O}_j$, $i,j \in \{1,2,\dots,N_l\}$, $i \neq j$, the sum of each row of $\mathcal{L}_{g_{ij}}^{\sigma(t)}$ is equal to zero.

Lemma 1 ([18]). *Under Assumptions 4–6, all eigenvalues of $\mathcal{L}_1^{\sigma(t)}$ have positive real parts, and $-(\mathcal{L}_1^{\sigma(t)})^{-1}\mathcal{L}_2^{\sigma(t)}$ has the following form*

$$-(\mathcal{L}_1^{\sigma(t)})^{-1}\mathcal{L}_2^{\sigma(t)} = \begin{bmatrix} \mathbf{1}_{g_1} & \mathbf{0}_{g_1} & \cdots & \mathbf{0}_{g_1} \\ \mathbf{0}_{g_2} & \mathbf{1}_{g_2} & \cdots & \mathbf{0}_{g_2} \\ \vdots & \vdots & \ddots & \vdots \\ \mathbf{0}_{g_{N_l}} & \mathbf{0}_{g_{N_l}} & \cdots & \mathbf{1}_{g_{N_l}} \end{bmatrix}.$$

Lemma 2 ([20]). *Under Assumptions 4–6, there is a real diagonal matrix $\mathcal{D}^{\sigma(t)} = \mathrm{diag}\{d_1^{\sigma(t)},\dots,d_M^{\sigma(t)}\}$ with $d_i^{\sigma(t)} > 0$, $i = 1,\dots,N_f$, such that $\mathcal{D}^{\sigma(t)}\mathcal{L}_1^{\sigma(t)} + (\mathcal{L}_1^{\sigma(t)})^\top\mathcal{D}^{\sigma(t)} > 0$.*

Remark 2. Assumptions 1–3 are fairly standard in the formation tracking for HMASs [13–15]. Assumptions 4–6 are commonly employed for group cooperative control problems [18–21,26–28].

Remark 3. Compared to the results on the format of time-varying formation shape in [11,13,18–20], which require the input matrix of the followers to be full column rank, the format (6) presented in this paper, which is based on the output regulation strategy, does not require this condition. This format not only features a simple structure but also allows the time-varying formation shape to be designed independently.

3. Main results

In this section, the distributed observer for the followers will be presented. Then, the GFTC protocols will be given.

3.1. Distributed observer

As the states of the leaders might not be accessible to all followers, it is essential to develop distributed observers by utilizing the information from neighboring agents to estimate the state of the leader in each subgroup.

For each follower in any subgroup $\mathcal{O}_q = \{\text{leader } q, \mathcal{O}_{fq}\}$, $k = 1,\dots,N_l$, the following distributed observer is given,

$$\dot{\boldsymbol{\eta}}_i = \boldsymbol{A}_0\boldsymbol{\eta}_i - \mu\boldsymbol{P}_0\boldsymbol{\delta}_i, \tag{7a}$$

$$\boldsymbol{\delta}_i = \sum_{k=1}^{N_l} a_{i0k}^{\sigma(t)}\left(\boldsymbol{\eta}_i - \boldsymbol{x}_{0k}\right) + \sum_{j=1}^{N_f} a_{ij}^{\sigma(t)}\left(\boldsymbol{\eta}_i - \boldsymbol{\eta}_j\right), \tag{7b}$$

where $\boldsymbol{\eta}_i$ is the state of the distributed observer, $\boldsymbol{\delta}_i$ denotes the neighboring relative estimation errors, $\mu > 0$ is a constant, and $\boldsymbol{P}_0$ is a real positive definite matrix to be determined later.

Then, the following theorem on the proposed distributed observer is presented.

Theorem 1. *Consider the distributed observer (7) under Assumptions 4–6. Let μ, $\boldsymbol{P}_0$, and the average dwell time $\bar{\tau}_d$ be chosen such that*

1. $\mu \geq \max\left\{\frac{\lambda_{\max}(\boldsymbol{D}^{\sigma(t)})}{\lambda_{\min}(\boldsymbol{\Phi}^{\sigma(t)})}\right\}$ $(\sigma(t) \in \{1,\dots,s\})$,
2. $\boldsymbol{P}_0\boldsymbol{A}_0 + \boldsymbol{A}_0^\top\boldsymbol{P}_0 - \boldsymbol{P}_0^2 + \mathrm{I}_{n_0} = 0$,
3. $\bar{\tau}_d > \frac{\ln\alpha}{\rho}$,

where $\boldsymbol{\Phi}^{\sigma(t)} = \mathcal{D}^{\sigma(t)}\mathcal{L}_1^{\sigma(t)} + (\mathcal{L}_1^{\sigma(t)})^\top\mathcal{D}^{\sigma(t)}$, $\rho = \frac{1}{\lambda_{\max}(\mathbf{P}_0)}$, and $\alpha = \max\left\{\frac{\lambda_{\max}(\boldsymbol{D}^m)}{\lambda_{\min}(\boldsymbol{D}^n)}\right\}$ $(m,n \in \{1,\dots,s\})$. Then, for each follower in any subgroup $\mathcal{O}_q = \{\text{leader } q, \mathcal{O}_{fq}\}$, $\lim_{t\to+\infty}\|\boldsymbol{\eta}_i(t) - \boldsymbol{x}_{0q}(t)\| = 0$.

Proof. Let $\tilde{\boldsymbol{\eta}}_i = \boldsymbol{\eta}_i - \boldsymbol{x}_{0q}$. From (2) and (7), one has

$$\dot{\tilde{\boldsymbol{\eta}}}_i = \boldsymbol{A}_0\tilde{\boldsymbol{\eta}}_i - \mu\boldsymbol{P}_0\boldsymbol{\delta}_i. \tag{8}$$

Let $\tilde{\boldsymbol{\eta}} = [\tilde{\boldsymbol{\eta}}_1^\top,\dots,\tilde{\boldsymbol{\eta}}_{N_f}^\top]^\top$, $\boldsymbol{x}_0 = [\boldsymbol{x}_{01}^\top,\dots,\boldsymbol{x}_{0N_l}^\top]^\top$, $\boldsymbol{\eta} = [\boldsymbol{\eta}_1^\top,\dots,\boldsymbol{\eta}_{N_f}^\top]^\top$, and $\boldsymbol{\delta} = [\boldsymbol{\delta}_1^\top,\dots,\boldsymbol{\delta}_M^\top]^\top$. From Lemma 1, one has $\tilde{\boldsymbol{\eta}} = \boldsymbol{\eta} + \left(\left((\mathcal{L}_1^{\sigma(t)})^{-1}\mathcal{L}_2^{\sigma(t)}\right)\otimes\mathrm{I}_{n_0}\right)\boldsymbol{x}_0$ and $\boldsymbol{\delta} = (\mathcal{L}_1^{\sigma(t)}\otimes\mathrm{I}_{n_0})\boldsymbol{\eta} + (\mathcal{L}_2^{\sigma(t)}\otimes\mathrm{I}_{n_0})\boldsymbol{x}_0 = (\mathcal{L}_1^{\sigma(t)}\otimes\mathrm{I}_{n_0})\tilde{\boldsymbol{\eta}}$. It then follows that the compact form of (8) can be rewritten as follows,

$$\dot{\tilde{\boldsymbol{\eta}}} = \left(\mathrm{I}_M\otimes\boldsymbol{A}_0 - \mu\left(\mathcal{L}_1^{\sigma(t)}\otimes\boldsymbol{P}_0\right)\right)\tilde{\boldsymbol{\eta}}. \tag{9}$$

Consider the following piecewise Lyapunov-like function

$$V = \tilde{\boldsymbol{\eta}}^\top(\mathcal{D}^{\sigma(t)}\otimes\boldsymbol{P}_0)\tilde{\boldsymbol{\eta}}. \tag{10}$$

It can be seen that $\boldsymbol{D}^{\sigma(t)}$ keeps fixed on each interval $[t_h, t_{h+1})$. Then, calculating the time derivative of (10) along the trajectory of (9) in each interval $[t_h, t_{h+1})$, one has

$$\begin{aligned}\dot{V} =&\tilde{\boldsymbol{\eta}}^{\top}\left(\boldsymbol{D}^{\sigma(t)}\otimes\left(\boldsymbol{P}_0\boldsymbol{A}_0+\boldsymbol{A}_0^{\top}\boldsymbol{P}_0-\boldsymbol{P}_0^2\right)\right)\tilde{\boldsymbol{\eta}}\\&+\tilde{\boldsymbol{\eta}}^{\top}\left((\boldsymbol{D}^{\sigma(t)}-\mu\boldsymbol{\Phi}^{\sigma(t)})\otimes\boldsymbol{P}_0^2\right)\tilde{\boldsymbol{\eta}}.\end{aligned}\tag{11}$$

Note that $\mu \geq \max\left\{\frac{\lambda_{\max}(\boldsymbol{D}^{\sigma(t)})}{\lambda_{\min}(\boldsymbol{\Phi}^{\sigma(t)})}\right\}$ $(\sigma(t)\in\{1,2,\ldots,s\})$ and $\boldsymbol{P}_0\boldsymbol{A}_0+\boldsymbol{A}_0^{\top}\boldsymbol{P}_0-\boldsymbol{P}_0^2+\mathrm{I}_{n_0}=0$. Then, from (11), one can obtain that

$$\dot{V}\leq-\tilde{\boldsymbol{\eta}}^{\top}\left(\boldsymbol{D}^{\sigma(t)}\otimes\mathrm{I}_{n_0}\right)\tilde{\boldsymbol{\eta}}\leq-\rho V(t).\tag{12}$$

Based on (12), one has

$$V(t_{h+1}^{-})\leq e^{-\rho(t_{h+1}-t_h)}V(t_h).\tag{13}$$

Via (10), one can obtain that $\lambda_{\min}\left(\boldsymbol{D}^{\sigma(t)}\right)\tilde{\boldsymbol{\eta}}^{\top}(\mathrm{I}_M\otimes\boldsymbol{P}_0)\tilde{\boldsymbol{\eta}}\leq V\leq\lambda_{\max}\left(\boldsymbol{D}^{\sigma(t)}\right)\tilde{\boldsymbol{\eta}}^{\top}(\mathrm{I}_M\otimes\boldsymbol{P}_0)\tilde{\boldsymbol{\eta}}$. It follows from Lemma 1 that $\tilde{\eta}$ is continuous over $[t_1,+\infty)$. Recalling that $\alpha=\max\left\{\frac{\lambda_{\max}(\boldsymbol{D}_m)}{\lambda_{\min}(\boldsymbol{D}_n)}\right\}$ $(m,n\in\{1,\ldots,s\})$, one can obtain that

$$V(t_{h+1})\leq\alpha V(t_{h+1}^{-}).\tag{14}$$

It then follows from (13) and (14) that

$$V(t_{h+1})\leq\alpha e^{-\rho(t_{h+1}-t_h)}V(t_h).\tag{15}$$

For any given time t within the interval $[t_{h+1}, t_{h+2})$, by employing the recursion approach, it can be derived from (15) that

$$V(t)\leq e^{-\rho(t-t_{h+1})}V(t_{h+1})\leq\alpha^k e^{-\rho(t-t_1)}V(t_1).\tag{16}$$

Via Definition 1, we have $k\leq N_0+\frac{t-t_1}{\bar{\tau}_d}$. Then, from (16), one can obtain that

$$\begin{aligned}V(t)\leq&\,\alpha^{\frac{t-t_1}{\bar{\tau}_d}}e^{-\rho(t-t_1)}\alpha^{N_0}V(t_1)\\=&\,e^{-(\rho-\frac{\ln\alpha}{\bar{\tau}_d})(t-t_1)}\alpha^{N_0}V(t_1).\end{aligned}\tag{17}$$

Since the average dwell time $\bar{\tau}_d>\frac{\ln\alpha}{\rho}$, it can be derived from (17) that $\lim_{t\to+\infty}\|\tilde{\boldsymbol{\eta}}(t)\|=0$. Thus, for each follower in any subgroup $\mathcal{O}_q=\{\text{leader } q,\mathcal{O}_{fq}\}$, $q=1,\ldots,N_l$, $\lim_{t\to+\infty}\|\boldsymbol{\eta}_i(t)-\boldsymbol{x}_{0k}(t)\|=0$. The proof is thus completed. □

Remark 4. Since $(\boldsymbol{A}_0,\mathrm{I}_{n_0})$ is controllable, there exists a unique solution $\boldsymbol{P}_0$ to the algebraic Riccati equation stated in Theorem 1.

3.2. Time-varying GFTC protocol

The GFTC protocol is constructed as follows:

$$\boldsymbol{u}_i=\boldsymbol{K}_{1i}\hat{\boldsymbol{x}}_i+\boldsymbol{K}_{2i}\eta_i+\boldsymbol{K}_{3i}\boldsymbol{h}_{xi},\tag{18a}$$

$$\dot{\hat{\boldsymbol{x}}}_i=\boldsymbol{A}_i\hat{\boldsymbol{x}}_i+\boldsymbol{B}_i\boldsymbol{u}_i+\boldsymbol{L}_i(\boldsymbol{C}_i\hat{\boldsymbol{x}}_i-\boldsymbol{y}_i),\tag{18b}$$

where $\hat{\boldsymbol{x}}_i$ is the state of the Luenberger observer, η_i is the state of the distributed observer, $\boldsymbol{K}_{1i}$, $\boldsymbol{K}_{2i}$, $\boldsymbol{K}_{3i}$, and $\boldsymbol{L}_i$ are matrices to be determined later.

Theorem 2. *Suppose that Assumptions 1–6 hold. Let $\boldsymbol{K}_{1i}$ and $\boldsymbol{L}_i$ be chosen such that $\boldsymbol{A}_i+\boldsymbol{B}_i\boldsymbol{K}_{1i}$ and $\boldsymbol{A}_i+\boldsymbol{L}_i\boldsymbol{C}_i$ are Hurwitz. $\boldsymbol{K}_{2i}$ and $\boldsymbol{K}_{3i}$ can be design as $\boldsymbol{K}_{2i}=\boldsymbol{U}_i-\boldsymbol{K}_{1i}\boldsymbol{X}_i$ and $\boldsymbol{K}_{3i}=\boldsymbol{U}_{Fi}-\boldsymbol{K}_{1i}\boldsymbol{X}_{Fi}$, where $(\boldsymbol{U}_i,\boldsymbol{X}_i)$ and $(\boldsymbol{U}_{Fi},\boldsymbol{X}_{Fi})$ are the solutions of (5) and (6), respectively. Then, the GFTC problem with switching topologies described by (4) is addressed under the distributed protocol (18).*

Proof. For any subgroup $\mathcal{O}_q=\{\text{leader } q,\mathcal{O}_{fq}\}$, $q=1,\ldots,N_l$, let $\boldsymbol{e}_i=\boldsymbol{x}_i-\boldsymbol{X}_i\boldsymbol{x}_{0q}-\boldsymbol{X}_{Fi}\boldsymbol{h}_{xi}$. It follows from (1), (2), (7), and (18) that

$$\dot{\boldsymbol{e}}_i=\left(\boldsymbol{A}_i+\boldsymbol{B}_i\boldsymbol{K}_{1i}\right)\boldsymbol{e}_i+\boldsymbol{B}_i\boldsymbol{K}_{2i}\tilde{\boldsymbol{\eta}}_i+\boldsymbol{B}_i\boldsymbol{K}_{1i}\tilde{\boldsymbol{x}}_i,\tag{19a}$$

$$\dot{\tilde{\boldsymbol{x}}}_i=(\boldsymbol{A}_i+\boldsymbol{L}_i\boldsymbol{C}_i)\tilde{\boldsymbol{x}}_i,\tag{19b}$$

where $\tilde{\boldsymbol{\eta}}_i=\boldsymbol{\eta}_i-\boldsymbol{x}_{0q}$ and $\tilde{\boldsymbol{x}}_i=\hat{\boldsymbol{x}}_i-\boldsymbol{x}_i$.

Since $\boldsymbol{A}_i+\boldsymbol{L}_i\boldsymbol{C}_i$ is Hurwitz, via (19b), one can obtain that $\lim_{t\to+\infty}\|\tilde{\boldsymbol{x}}_i(t)\|=0$ exponentially. Note that $\lim_{t\to+\infty}\|\tilde{\boldsymbol{\eta}}_i(t)\|=0$ and $\boldsymbol{A}_i+\boldsymbol{B}_i\boldsymbol{K}_{1i}$ is Hurwitz, it then follows from (19) that $\lim_{t\to+\infty}\|\boldsymbol{e}_i(t)\|=0$. Moreover, since $\boldsymbol{e}_{yi}=\boldsymbol{C}_i\boldsymbol{e}_i=\boldsymbol{y}_i-\boldsymbol{h}_{yi}-\boldsymbol{y}_{0q}$, one has $\lim_{t\to+\infty}\|\boldsymbol{e}_{yi}(t)\|=0$, which means the GFTC problem with switching topologies described by (4) is addressed. The proof is thus completed. □

Remark 5. The convergence rate of $e_i(t)$ is dependent on the maximum real part of the eigenvalues of $\boldsymbol{A}_i+\boldsymbol{B}_i\boldsymbol{K}_{1i}$, the maximum real part of the eigenvalues of $\boldsymbol{A}_i+\boldsymbol{L}_i\boldsymbol{C}_i$, and the convergence rate of the distributed observer error. By choosing different gain matrices $\boldsymbol{K}_{1i}$ and $\boldsymbol{L}_i$, the eigenvalues of the matrices $\boldsymbol{A}_i+\boldsymbol{B}_i\boldsymbol{K}_{1i}$ and $\boldsymbol{A}_i+\boldsymbol{L}_i\boldsymbol{C}_i$ can be placed to different locations, thereby affecting the convergence rate of the group formation tracking error.

Remark 6. A sufficient condition for achieving the desired group formation tracking under switching topologies is that the average dwell time of the switching signal satisfies $\bar{\tau}_d>\frac{\ln\alpha}{\rho}$. If this condition is satisfied, our proposed method can solve the GFTC problem; otherwise, our method cannot guarantee the achievement of the desired group formation tracking.

4. Simulation

This section gives a simulation to illustrate the effectiveness of the theoretical result.

The HMAS is divided into three groups, each led by a single leader. The first two groups each consist of one leader and three followers, while the third group includes one leader and four followers. The switching topologies are given in Fig. 2.

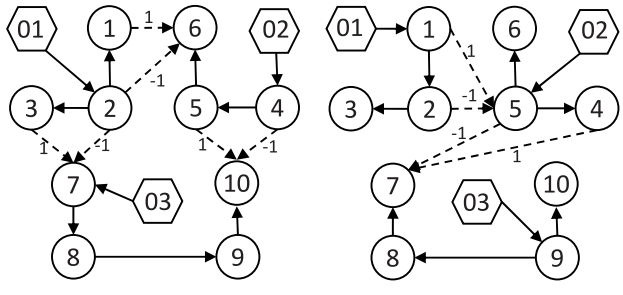

Fig. 2. Switching topologies $\mathcal{G}^{\sigma(t)}$ with $\sigma(t)\in\{1,2\}$.

The system matrices of the followers adopted from [13] are given by

$$\boldsymbol{A}_i=\mathrm{I}_2\otimes\begin{bmatrix}0&1\\\alpha_i&\beta_i\end{bmatrix},\boldsymbol{B}_i=\mathrm{I}_2\otimes\begin{bmatrix}0\\1\end{bmatrix},\boldsymbol{C}_i=\mathrm{I}_2\otimes[1\ 0],$$

$$\boldsymbol{A}_j=\mathrm{I}_2\otimes 0,\boldsymbol{B}_j=\mathrm{I}_2,\boldsymbol{C}_j=\mathrm{I}_2,$$

where $i=\{1,\ldots,8\}$, $j=\{9,10\}$, the parameters $\{\alpha_i,\beta_i\}$ are set as $\{-2\ -4\}$, $\{-1\ -2\}$, $\{-3\ -5\}$, $\{-3\ -3\}$, $\{-1\ -1\}$, $\{-2\ -2\}$, $\{-4\ -4\}$, and $\{-5\ -5\}$.

The system matrices of the leaders are given as follows:

$$\boldsymbol{A}_0=\mathrm{I}_2\otimes\begin{bmatrix}0&1\\0&0\end{bmatrix},\boldsymbol{C}_0=\mathrm{I}_2\otimes[1\ 0].$$

The time-varying formation vectors for each group are denoted as

$$\boldsymbol{h}_{xp}(t) = 15\begin{bmatrix} \sin\left(t+\frac{(p-1)2\pi}{3}\right) \\ \cos\left(t+\frac{(p-1)2\pi}{3}\right) \\ \cos\left(t+\frac{(p-1)2\pi}{3}\right) \\ -\sin\left(t+\frac{(p-1)2\pi}{3}\right) \end{bmatrix},\ p=1,2,3,$$

$$\boldsymbol{h}_{xq}(t) = 10\begin{bmatrix} \sin\left(t+\frac{(q-4)2\pi}{3}\right) \\ \cos\left(t+\frac{(q-4)2\pi}{3}\right) \\ \cos\left(t+\frac{(q-4)2\pi}{3}\right) \\ -\sin\left(t+\frac{(q-4)2\pi}{3}\right) \end{bmatrix},\ q=4,5,6,$$

$$\boldsymbol{h}_{xr}(t) = 15\begin{bmatrix} \sin\left(t+\frac{(r-7)\pi}{2}\right) \\ \cos\left(t+\frac{(r-7)\pi}{2}\right) \\ \cos\left(t+\frac{(r-7)\pi}{2}\right) \\ -\sin\left(t+\frac{(r-7)\pi}{2}\right) \end{bmatrix},\ r=7,8,9,10,$$

and $\boldsymbol{C}_F = \mathrm{I}_2 \otimes \begin{bmatrix}1 & 0\end{bmatrix}$. Solving the regulator Eqs. (5) and (6) yields

$$\boldsymbol{X}_i = \mathrm{I}_2 \otimes \begin{bmatrix}1 & 0\\ 0 & 1\end{bmatrix}, \boldsymbol{U}_i = \mathrm{I}_2 \otimes \begin{bmatrix}-\alpha_i & -\beta_i\end{bmatrix},$$

$$\boldsymbol{X}_j = \mathrm{I}_2 \otimes \begin{bmatrix}1 & 0\end{bmatrix}, \boldsymbol{U}_j = \mathrm{I}_2 \otimes \begin{bmatrix}0 & 1\end{bmatrix},$$

$$\boldsymbol{X}_{Fi} = \mathrm{I}_2 \otimes \begin{bmatrix}1 & 0\\ 0 & 1\end{bmatrix}, \boldsymbol{U}_{Fi} = \mathrm{I}_2 \otimes \begin{bmatrix}-1-\alpha_i & -\beta_i\end{bmatrix},$$

$$\boldsymbol{X}_{Fj} = \mathrm{I}_2 \otimes \begin{bmatrix}1 & 0\end{bmatrix}, \boldsymbol{U}_{Fj} = \mathrm{I}_2 \otimes \begin{bmatrix}0 & 1\end{bmatrix}.$$

It can be derived from Theorem 1 that the average dwell time $\bar{\tau}_d > 7.3958$ s. Therefore, the switching period between $\mathcal{G}^1$ and $\mathcal{G}^2$ can be set as 10 s. Define $\boldsymbol{P}_0 = \mathrm{I}_2 \otimes \begin{bmatrix}0.9102 & 0.4142\\ 0.4142 & 1.2872\end{bmatrix}$ and $\mu = 25$. Select $\boldsymbol{K}_{11} = \mathrm{I}_2 \otimes [1.5\ 2.5]$, $\boldsymbol{K}_{12} = \mathrm{I}_2 \otimes [0.5\ 0.5]$, $\boldsymbol{K}_{13} = \mathrm{I}_2 \otimes [2.5\ 3.5]$, $\boldsymbol{K}_{14} = \mathrm{I}_2 \otimes [2.5\ 1.5]$, $\boldsymbol{K}_{15} = \mathrm{I}_2 \otimes [0.5\ -0.5]$, $\boldsymbol{K}_{16} = \mathrm{I}_2 \otimes [1.5\ 0.5]$, $\boldsymbol{K}_{17} = \mathrm{I}_2 \otimes [3.5\ 2.5]$, $\boldsymbol{K}_{18} = \mathrm{I}_2 \otimes [4.5\ 3.5]$, $\boldsymbol{K}_{19} = \mathrm{I}_2 \otimes -0.5$, $\boldsymbol{K}_{110} = \mathrm{I}_2 \otimes -0.5$, $\boldsymbol{L}_1 = \mathrm{I}_2 \otimes [2.5\ -8.5]^\top$, $\boldsymbol{L}_2 = \mathrm{I}_2 \otimes [0.5\ -0.5]^\top$, $\boldsymbol{L}_3 = \mathrm{I}_2 \otimes [3.5\ -15]^\top$, $\boldsymbol{L}_4 = \mathrm{I}_2 \otimes [1.5\ -2]^\top$, $\boldsymbol{L}_5 = \mathrm{I}_2 \otimes [-0.5\ 1]^\top$, $\boldsymbol{L}_6 = \mathrm{I}_2 \otimes [0.5\ 0.5]^\top$, $\boldsymbol{L}_7 = \mathrm{I}_2 \otimes [2.5\ -6.5]^\top$, $\boldsymbol{L}_8 = \mathrm{I}_2 \otimes [3.5\ -13]^\top$, $\boldsymbol{L}_9 = \mathrm{I}_2 \otimes -0.5$, $\boldsymbol{L}_{10} = \mathrm{I}_2 \otimes -0.5$, $\boldsymbol{K}_{2i} = \mathrm{I}_2 \otimes [0.5\ 1.5]$, $\boldsymbol{K}_{2j} = \mathrm{I}_2 \otimes [0.5\ 1]$, $\boldsymbol{K}_{3i} = \mathrm{I}_2 \otimes [-0.5\ 1.5]$, $\boldsymbol{K}_{3j} = \mathrm{I}_2 \otimes [0.5\ 1]$ with $i = 1, \ldots 8$ and $j = 9, 10$. The initial states of the followers are randomly generated within the range of -5 to 5. The initial states of the leaders are set as $[\Theta\ -1\ \Theta\ 1]^\top$, $[\Theta\ 1\ \Theta\ -1]^\top$, and $[\Theta\ 1\ \Theta\ 1]^\top$ with Θ a random value between $(-0.5, 0.5)$. The initial states of the distributed observer are set as $\mathbf{0}_4$.

Simulation results are presented in Figs. 3–5. Fig. 3 depicts the output trajectory of the HMAS over the simulation period. Here, groups one to three are color-coded as red, green, and blue, respectively, with pentagram markers indicating the leaders and circles representing the followers. It can be seen from Fig. 3 that the HMAS is divided into three distinct groups, with the followers of each group successfully forming the desired formation and tracking their respective leader. Fig. 4 illustrates the group formation tracking errors. It can be observed that $\lim_{t\to+\infty} \|\boldsymbol{e}_{yi}(t)\| = 0$. Additionally, it can be seen from Fig. 5 that $\lim_{t\to+\infty} \|\boldsymbol{\eta}(t)\| = 0$. This indicates that the states of the distributed observer (7) tend to the state of the leader in each subgroup as time goes to infinity.

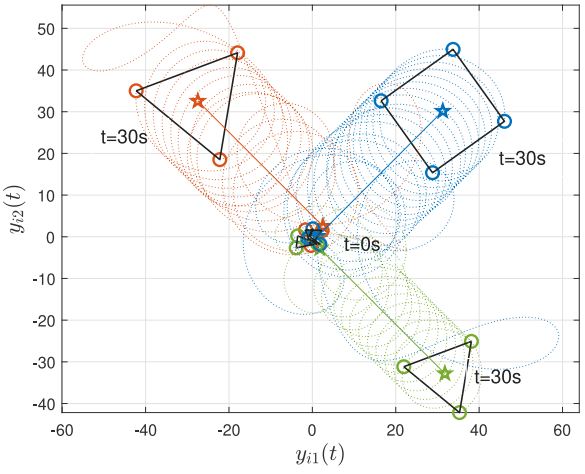

Fig. 3. Output trajectories.

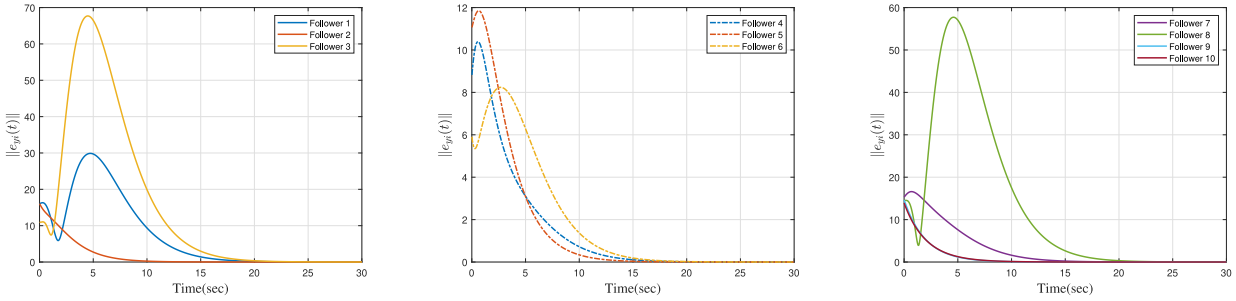

(a) (b) (c)

Fig. 4. The group formation tracking errors: (a) Subgroup 1; (b) Subgroup 2; (c) Subgroup 3.

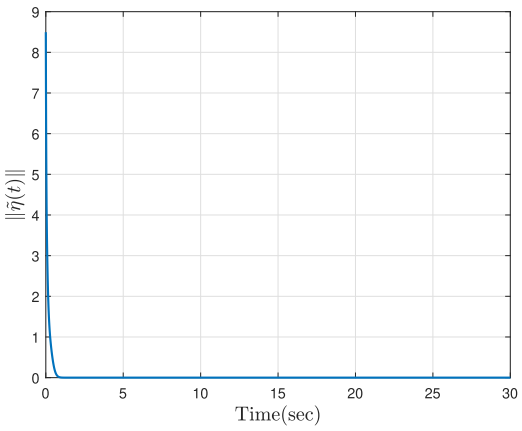

Fig. 5. The distributed observer error.

5. Conclusion

This paper investigates the time-varying output GFTC problem for HMASs under switching topologies. We have designed distributed observers that enable the followers to estimate the states of the leaders for each group under switching topologies. Then, an observed-based GFTC protocol is developed. Based on piecewise Lyapunov stability theory, the threshold for the average dwell time associated with the switching topologies has been established, and the convergence of both distributed observer error and GFTC error has been proven. The effectiveness of the proposed control strategy has been verified through a simulation example. In the future, we will investigate the GFTC problem for HMASs under jointly connected digraphs and the finite-time GFTC problem. Additionally, it is interesting to study the robust GFTC problem for HMASs subject to external disturbances or other uncertainties.

CRediT authorship contribution statement

Shiyu Zhou: Writing – original draft, Validation, Methodology, Investigation. **Dong Sun:** Writing – review & editing, Funding acquisition.

Declaration of competing interest

The authors declare that they have no known competing financial interests or personal relationships that could have appeared to influence the work reported in this paper.

Data availability

Data will be made available on request.

References

[1] R. Olfati-Saber, R.M. Murray, Distributed cooperative control of multiple vehicle formations using structural potential functions, IFAC Proc. Vol. 35 (1) (2002) 495–500.
[2] K.-K. Oh, M.-C. Park, H.-S. Ahn, A survey of multi-agent formation control, Automatica 53 (2015) 424–440.
[3] X. Huang, Z. Li, F.L. Lewis, Cost-effective distributed FTFC for uncertain nonholonomic mobile robot fleet with collision avoidance and connectivity preservation, J. Autom. Intell. 2 (1) (2023) 42–50.
[4] W. Ren, Consensus strategies for cooperative control of vehicle formations, IET Control Theory Appl. 1 (2) (2007) 505–512.
[5] J.A. Fax, R.M. Murray, Information flow and cooperative control of vehicle formations, IEEE Trans. Autom. Control 49 (9) (2004) 1465–1476.
[6] W. Ren, R.W. Beard, Consensus seeking in multiagent systems under dynamically changing interaction topologies, IEEE Trans. Autom. Control 50 (5) (2005) 655–661.
[7] T. Liu, Z.-P. Jiang, Distributed formation control of nonholonomic mobile robots without global position measurements, Automatica 49 (2) (2013) 592–600.
[8] M. Porfiri, D.G. Roberson, D.J. Stilwell, Tracking and formation control of multiple autonomous agents: A two-level consensus approach, Automatica 43 (8) (2007) 1318–1328.
[9] W. Wang, J. Huang, C. Wen, H. Fan, Distributed adaptive control for consensus tracking with application to formation control of nonholonomic mobile robots, Automatica 50 (4) (2014) 1254–1263.
[10] S. Zhao, Z. Li, Z. Ding, Bearing-only formation tracking control of multi-agent systems, IEEE Trans. Autom. Control 64 (11) (2019) 4541–4554.
[11] X. Dong, Q. Li, Z. Ren, Time-varying group formation analysis and design for general linear multi-agent systems with directed topologies, Internat. J. Robust Nonlinear Control 27 (9) (2017) 1640–1652.
[12] Y. Hua, X. Dong, Q. Li, Z. Ren, Distributed time-varying formation robust tracking for general linear multiagent systems with parameter uncertainties and external disturbances, IEEE Trans. Cybern. 47 (8) (2017) 1959–1969.
[13] Y. Hua, X. Dong, G. Hu, Q. Li, Z. Ren, Distributed time-varying output formation tracking for heterogeneous linear multi-agent systems with a nonautonomous leader of unknown input, IEEE Trans. Autom. Control 64 (10) (2019) 4292–4299.
[14] W. Jiang, G. Wen, Z. Peng, T. Huang, A. Rahmani, Fully distributed formation-containment control of heterogeneous linear multiagent systems, IEEE Trans. Autom. Control 64 (9) (2018) 3889–3896.
[15] B. Wang, W. Chen, B. Zhang, P. Shi, H. Zhang, A nonlinear observer-based approach to robust cooperative tracking for heterogeneous spacecraft attitude control and formation applications, IEEE Trans. Autom. Control 68 (1) (2022) 400–407.
[16] W. Wu, W. Zhou, T. Chen, Cluster synchronization of linearly coupled complex networks under pinning control, IEEE Trans. Circuits Syst. I. Regul. Pap. 56 (4) (2008) 829–839.
[17] W. Xia, M. Cao, Clustering in diffusively coupled networks, Automatica 47 (11) (2011) 2395–2405.
[18] J. Hu, P. Bhowmick, A. Lanzon, Distributed adaptive time-varying group formation tracking for multi-agent systems with multiple leaders on directed graphs, IEEE Trans. Control. Netw. Syst. 7 (1) (2019) 140–150.
[19] X. Dong, Q. Li, Q. Zhao, Z. Ren, Time-varying group formation analysis and design for general linear multi-agent systems with directed topologies, Internat. J. Robust Nonlinear Control 27 (9) (2017) 1640–1652.
[20] Y. Lu, X. Dong, Q. Li, J. Lü, Z. Ren, Time-varying group formation-containment tracking control for general linear multiagent systems with unknown inputs, IEEE Trans. Cybern. 52 (10) (2021) 11055–11067.
[21] C.-D. Liang, M.-F. Ge, Z.-W. Liu, Y.-W. Wang, H.R. Karimi, Output multiformation tracking of networked heterogeneous robotic systems via finite-time hierarchical control, IEEE Trans. Cybern. 51 (6) (2020) 2893–2904.
[22] K. You, Z. Li, L. Xie, Consensus condition for linear multi-agent systems over randomly switching topologies, Automatica 49 (10) (2013) 3125–3132.
[23] G. Wen, W.X. Zheng, On constructing multiple Lyapunov functions for tracking control of multiple agents with switching topologies, IEEE Trans. Autom. Control 64 (9) (2018) 3796–3803.
[24] X. Dong, G. Hu, Time-varying formation control for general linear multi-agent systems with switching directed topologies, Automatica 73 (2016) 47–55.
[25] X. Dong, Y. Zhou, Z. Ren, Y. Zhong, Time-varying formation tracking for second-order multi-agent systems subjected to switching topologies with application to quadrotor formation flying, IEEE Trans. Ind. Electron. 64 (6) (2016) 5014–5024.
[26] J. Yu, L. Wang, Group consensus in multi-agent systems with switching topologies and communication delays, Systems Control Lett. 59 (6) (2010) 340–348.
[27] J. Qin, C. Yu, Cluster consensus control of generic linear multi-agent systems under directed topology with acyclic partition, Automatica 49 (9) (2013) 2898–2905.
[28] L. Tian, Y. Hua, X. Dong, J. Lü, Z. Ren, Distributed time-varying group formation tracking for multiagent systems with switching interaction topologies via adaptive control protocols, IEEE Trans. Ind. Informatics 18 (12) (2022) 8422–8433.
[29] J.P. Hespanha, A.S. Morse, Stability of switched systems with average dwell-time, in: Proceedings of the 38th IEEE Conference on Decision and Control, 1999, pp. 2655–2660.
[30] S. Li, J. Zhang, X. Li, F. Wang, X. Luo, X. Guan, Formation control of heterogeneous discrete-time nonlinear multi-agent systems with uncertainties, IEEE Trans. Ind. Electron. 64 (6) (2017) 4730–4740.
[31] X. Yu, L. Liu, Cooperative control for moving-target circular formation of nonholonomic vehicles, IEEE Trans. Autom. Control 62 (7) (2016) 3448–3454.
[32] Y. Hua, X. Dong, Q. Li, Z. Ren, Distributed adaptive formation tracking for heterogeneous multiagent systems with multiple nonidentical leaders and without well-informed follower, Internat. J. Robust Nonlinear Control 30 (6) (2020) 2131–2151.
[33] B. Yan, P. Shi, C.-C. Lim, Robust formation control for nonlinear heterogeneous multiagent systems based on adaptive event-triggered strategy, IEEE Trans. Autom. Sci. Eng. 19 (4) (2021) 2788–2800.

Shiyu Zhou received the B.Eng. degree in automation from Northwestern Polytechnical University, Xi'an, China, in 2019, and the M.Eng. degree in control science and engineering from the Beihang University, Beijing, China, in 2022. She is currently pursuing the Ph.D. degree in control science and engineering with the Department of Biomedical Engineering, City University of Hong Kong, Hong Kong.

Her current research interests include cooperative control of multiagent systems and synchronization of complex networks.

Dong Sun received the B.Eng. and M.Eng. degrees in precision instrument and mechanology from Tsinghua University, Beijing, China, in 1990 and 1994, respectively, and the Ph.D. degree in robotics and automation from The Chinese University of Hong Kong, Hong Kong, in 1997. He is a Chair Professor with the Department of Biomedical Engineering, City University of Hong Kong, Hong Kong, SAR, China.

Professor Sun is currently Fellow of the Canadian Academy of Engineering in Canada, Member of the European Academy of Sciences and Arts, Fellow of the International Academy of Medical and Biological Engineering, Fellow of the American Society of Mechanical Engineers.